SPE Brazil Flow Assurance Technology Congress
Rio de Janeiro, Brazil, November 06 – 08 2024

Detection and analysis of the Taylor bubble, Wake and Liquid slug with Wire-Mesh Sensor (WMS) in a Vertical Gas-Liquid Slug Flow

Carolina C. Rodrigues[1]*, Paul A. D. Maldonado[1], Clara L. Meinert[1], Eduardo N. dos Santos[1], Moises A. Marcelino Neto[1], Alain Liné[2], Rigoberto E. M. Morales[1]
[1]Multiphase Flow Research Center – NUEM, Federal Technological University of Parana, Brazil
[2]Toulouse Biotechnology Institute, Université de Toulouse, CNRS, INRAE, INSA, Toulouse, France
*carolcimarelli@gmail.com

Abstract
Slug flow is characterized by the alternate passage of two structures, the Taylor bubble and the liquid slug. Because of its transient and intermittent behavior, modeling this flow pattern constitutes a challenge. At the beginning of the liquid slug a recirculation region known as wake exists, whose behavior differ than from the rest of the liquid slug showing a higher gas fraction and higher pressure drop. This study experimentally characterizes slug flow with the use of two capacitive wire-mesh sensors in a 0.050-m ID, 15-m long vertical pipe, using air and water as working fluids. Gas and liquid superficial velocities ranged from 0.4 to 2.6 m/s. Preliminary results have shown that the gas fraction remain relatively constant with an increasing ratio between the Taylor bubble and the unit cell lengths (intermittence factor). The intermittence factor has a stronger impact on the Taylor bubble length than on the wake and liquid slug lengths.The Taylor bubble gas fraction remains constant with an increasing mixture velocity, while the wake and liquid slug gas fraction increase.

Keywords
Vertical-Slug-flow; Wire-Mesh-Sensor; Gas-fraction.

Introduction
Vertical slug flow occurs in a wide range of engineering applications. In the oil & gas industry, it occurs during the production and transportation of oil–gas mixtures, specifically in wells and production pipelines. In vertical pipelines, a large differential pressure exists in the liquid column. Consequently, the accurate prediction of the pressure drop and the spatial distribution of the phases in the pipeline is of utmost importance to design separators or to predict the flow behavior along the pipeline. The slug flow pattern is characterized by the intermittent passage of two structures: an elongated bubble, known as the Taylor bubble, followed by a liquid plug containing dispersed bubbles known as the liquid slug.

The literature contains different methodologies to simulate slug flows. Because of the flow intermittence, the first models assumed that the liquid and gas structures repeat in time and space, the so-called unit cell models [1, 2, 3]. A unit cell is composed of a liquid slug and an elongated bubble. The liquid slug may carry dispersed bubbles, whereas the elongated bubble flows surrounded by a film of liquid. The bubble region is generally modeled as a separate flow pattern, whereas the liquid slug can be regarded as a homogeneously dispersed bubbly flow pattern. Slug flow is hence treated as a series of identical unit cells traveling with a velocity that is equal to that of the translational bubble velocity. Considering a frame of reference moving with the elongated bubble velocity, the unit cell seems frozen in space and slug flow can be considered as a steady state phenomenon. This representation allows the calculation of hydrodynamic parameters in the unit cell and by extension in the overall flow. Taitel & Barnea [3] generalized the approach of [2, 4] for horizontal cases and [5, 6] for vertical configurations. These mechanistic models are still in use, because of their low computational cost. Transient models have also been developed. Some well-known models are the two-fluid [7], drift-flux [1] and slug tracking [8,9,10] ones.

All models for slug flow pattern depend on experimental data and closure relations. For the unit cell models the following parameters must be known or obtained through correlations: the translational bubble velocity (V_{TB}), the intermittence factor (β) or the gas fraction in the liquid slug (RGS). The intermittence factor is the ratio between the elongated bubble length (LB) and the unit cell length ($LU = LB + LS$). Another way to express β as a function of the gas fraction is:

$$\beta = \frac{LB}{LU} = \frac{RG - RGS}{RGB - RGS} \quad (1)$$

which can be achieved through the mass conservation equations. This parameter is important because a higher intermittence leads to a smaller pressure drop since most of it occurs in the liquid slug.

The liquid slug can be split into specific regions: the wake, the developing region or far wake and the fully developed [9, 11] regions. The influence of the wake on the pressure in horizontal flows was evaluated by [2, 4], considering that this pressure drop is associated with the acceleration of the slow-moving liquid in the film to the liquid velocity within the liquid slug. Collins et al. [12] proposed a correlation for the wake effect on the elongated bubble velocity for vertical flows. Studies using PIV measurements also analyzed the wake shape and the liquid recirculation for vertical flows [13]. The wake length (*LW*) was also evaluated by [9, 14] and a correlation for *LW* was proposed by [14]. Nevertheless, the wake is usually ignored in modeling as it is considered as part of the liquid slug, whose several correlations in the literature lack consensus among them. This raises the question on whether the wake should be considered as part of the liquid slug or as part of the Taylor bubble or even as a third region. In this sense, this article analyzes the gas fraction and lengths of the wake, Taylor bubble and liquid slug.

Methodology

The experimental study was developed in the Multiphase Flow Research Center (NUEM) at UTFPR with a 0.05-m ID pipe. A scheme of the two-phase flow facility is shown in Figure 1. Air and water were used as fluids at ambient temperature and pressure.

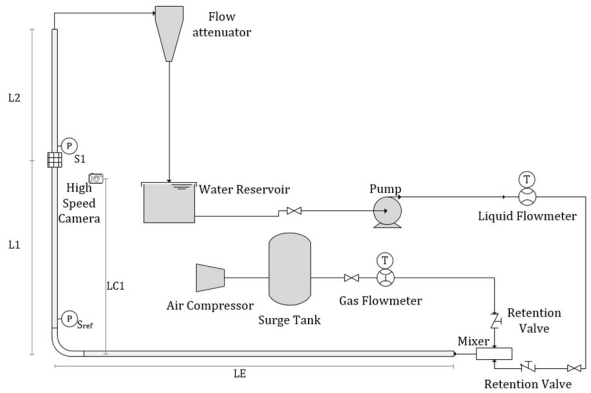

Figure 1. Schematic diagram of the multiphase flow loop facility.

Water is pumped from a reservoir by a positive displacement pump, which directs the liquid phase to the test section. In parallel, air is fed into the test section by the compressor through a surge tank. The air and the water streams combine in the mixer section at the beginning of the horizontal section (LE = 31 m) as a stratified flow pattern. The test section consists of a 15-m high vertical line. At the end of the horizontal line, a 90°-bend directs the flow into the vertical test section and finally into the cyclonic separator. The water returns to the tank and the air is released into the atmosphere.

Two Coriolis flowmeters were positioned in the beginning of each phase line, enabling the simultaneous monitoring of both phases. Two wire-mesh sensors were installed at 8 m height (160D) from the horizontal section (L1), separated by a distance of 50 mm (wire diameter 120 μm, frequency 2000 Hz). In this study, nine different combinations of air-water superficial velocities (JG and JL) were investigated (Table 1).

Table 1. Experimental envelope with its gas and liquid superficial velocities.

Case	JG [m/s]	JL [m/s]	J [m/s]	JG/JL
# 1	0.68	0.51	1.18	1.33
# 2	0.70	1.00	1.70	0.70
# 3	1.01	0.74	1.75	1.36
# 4	1.34	1.00	2.35	1.34
# 5	1.39	1.50	2.89	0.93
# 6	1.68	1.26	2.94	1.34
# 7	1.97	1.00	2.97	1.96
# 8	2.05	1.49	3.54	1.37
# 9	2.59	1.00	3.60	2.59

Wire Mesh Sensor and data processing

The wire-mesh sensor (WMS) is an intrusive imaging device that provides flow images at high spatial and temporal resolutions. This sensor is a hybrid solution between an intrusive probe and a tomographic cross-sectional imaging [15].

The WMS consists of two perpendicular electrode planes, emitters and receivers, with an axial separation of 1.5 mm, that is, they are not in contact. The capacitance of the flowing media is measured in the gaps between all crossing points at high repetition rates, measuring the permittivity of the phases. The measurement setups consist of sixteen (16) stainless steel wires (electrodes) in each plane (16x16), distributed evenly along the pipe cross-section (3.125 mm).

From the WMS data, it was possible to identify and discriminate Taylor bubbles and liquid slugs. The Taylor bubbles are characterized by the high gas fractions in the time series signal whereas the low ones identify the liquid slug, the methodology can be found in detail in [15].

Detection of the Taylor bubble beginning and end, and of the wake end

The new detection of the slug flow unit cell was done considering three regions: the Taylor bubble, the wake, and the liquid slug. It was considered that the end of a liquid slug is the beginning of a new coming Taylor bubble, a Taylor bubble end is the beginning of a wake and the end of a wake is a new liquid slug beginning. To identify those regions three different views were evaluated from the WMS data as shown in Figure 2. The first graph is the average time series, followed by the gas fraction in three (3) strategical-cross-section regions. Each region was detected manually and compared with a 3D WMS detection as explained in [15]. In the first step of the detection, spherical caps were considered as bubbles and at least 100 Taylor bubbles per experimental point were identified after all the unit cells were pinpointed.

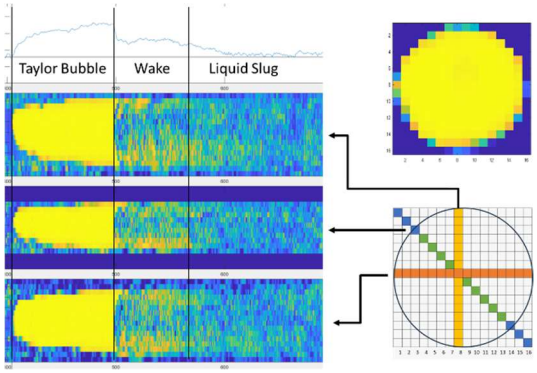

Figure 2. Detection of the Taylor bubble beginning and end, and of the wake end with WMS.

Results and Discussion

Discerning an elongated bubble from a spherical cap, trivial as it may seem, can be quite subjective. Barnea & Shemer [16], among others, assumed that elongated bubbles are the ones with a length of at least two pipe diameters (2D). Figure 3 shows the Taylor bubble gas fractions (*RGB*) using this criterion and, also, the gas fraction of the following wake (*RGW*) and liquid slug (*RGS*).

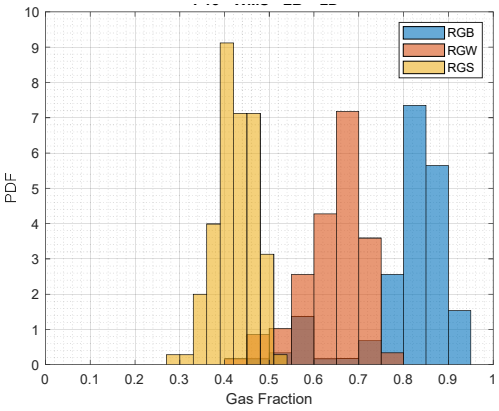

Figure 3. Gas fraction PDF of the Taylor bubble (*RGB*), wake (*RGW*) and liquid slug (*RGS*) for all the unit cell with *LB* > 2D.

Figure 3 shows some degree of overlapping between *RGB* and *RGW*, and a few RGB values smaller than 0.7, which is inconsistent with a typical Taylor bubble behavior. This could indicate that the length is not sufficient to tell Taylor bubbles from spherical caps. Other filters were tested and the one with better results was *LB* > 4D and *RGB* > 0.7, as shown in Figure 4.

Figure 5 shows the gas fraction as a function of the bubble length for the filters: *RGB* > 0.7 and *LB* > 4D, *RGB* > 0.6 and 2D < *LB* < 4D, where "the rest" refers to the spherical caps. From the image it is possible to observe that the gas fraction for *RGB* > 0.7 and *LB* > 4D is almost constant for *LB* > 20D.

A mass balance verification was done in Figure 6. It is possible to observe that the mass conservation is kept within ±10% deviation.

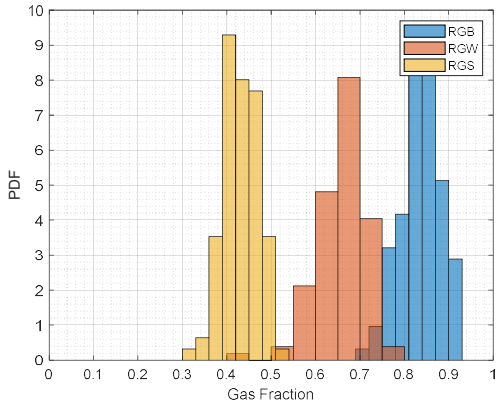

Figure 4. Gas fraction PDF of Taylor bubble (*RGB*), wake (*RGW*) and liquid slug (*RGS*) for all the unit cell with *LB* > 4D, *RGB* > 0.4.

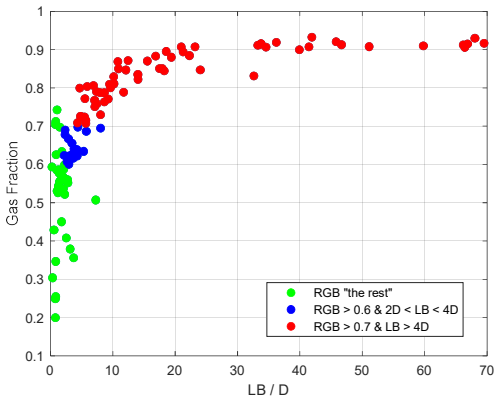

Figure 5. Gas fraction as a function of Taylor bubble length, *LB*, for different Taylor bubble filters: *RGB* > 0.7 and *LB* > 4D, *RGB* > 0.6 and 2D < *LB* < 4D, where "the rest" refers to the spherical caps.

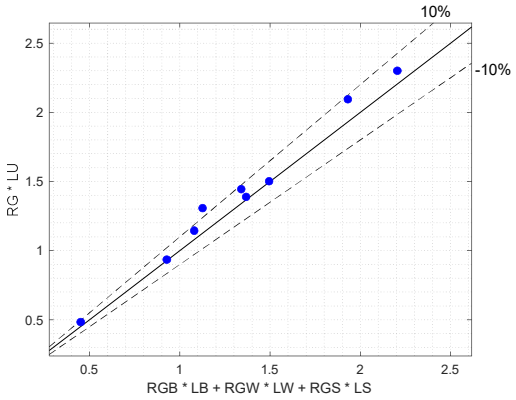

Figure 6. Comparison of gas mass balance in the unit cell with the sum of the individual gas masses in each of the three unit cell regions.

Figure 7 shows the influence of the mixture velocity (*J*) on *RGB*, *RGW* and *RGS*. It can be observed that *RGB* remains almost constant when *J* is increased, whereas *RGS* and *RGW* increase.

The influence of the intermittence factor on the gas fraction in the Taylor bubble (RGB), wake (RGW) and liquid slug (RGS) is shown in Figure 8. One can observe that the gas fraction remains roughly constant for all the range evaluated.

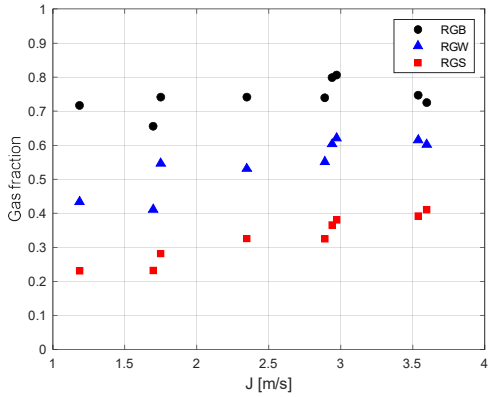

Figure 7. Influence of the mixture velocity (J) on the gas fraction of the Taylor bubble (RGB), wake (RGW) and liquid slug (RGS).

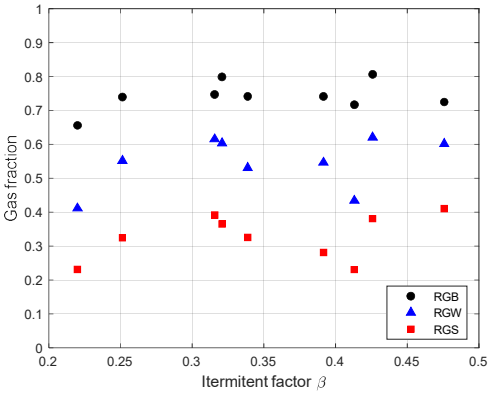

Figure 8. Influence of the intermittence factor (β) on the gas fraction in the Taylor bubble (RGB), wake (RGW) and liquid slug (RGS).

Figure 9 shows the influence of the intermittence factor (β) on the length of Taylor bubble (*LB*), wake (*LW*) and liquid slug (*LS*). From the image, it is clear that *LB* exhibits the greatest increase with an increasing β, even comparing with the other lengths (*LW* and *LS*).

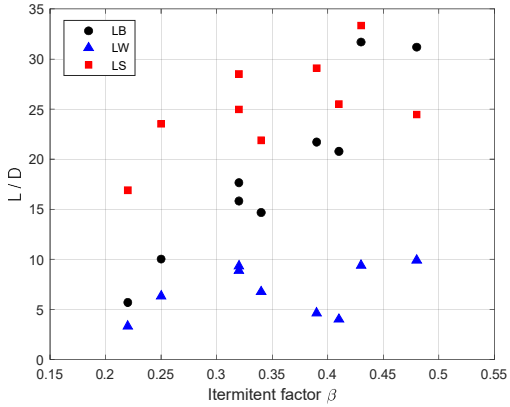

Figure 9. Influence of the intermittent factor (β) on the length of Taylor bubble (*LB*), wake (*LW*) and liquid slug (*LS*).

Conclusions

The objective of this work was to experimentally characterize the three regions in slug flow (Taylor bubble, wake, and liquid slug) in a vertical pipe. The experimental methodology described herein relied upon the use of an experimental circuit located at NUEM/UTFPR, with a 31-meter long horizontal pipe, followed by a 15-m height, 0.05-m vertical pipe, with air and water as fluids. Wire-mesh sensor was used to obtain the Taylor bubble velocities and the gas fraction. The test grid covered nine (9) flow combinations.

From the experimental data, the Taylor bubble, wake and liquid slug regions were identified. The gas fractions and lengths of each region were evaluated and compared with the experimental mixture velocity and with the intermittence factor. Increases in the gas fraction of the wake and liquid slug were observed when the mixture velocity was increased, while the gas fraction in the Taylor bubble remained constant. Results showed that the intermittency factor (β) did not affect the gas fraction of the Taylor bubble, wake and liquid slug, but the higher β, the longer the length of those regions. The length of the Taylor bubble exhibits the largest increase when compared with the other lengths (*LW* and *LS*). Further analyses must be performed to better understand the wake region and to propose a model for this region.

Acknowledgments

The authors would like to express their gratitude to NUEM, CAPES/DS, FUNTEF-PR and PRH21-ANP for their financial support.

Responsibility Notice

The authors are the only ones responsible for the paper content.

References

[1] Wallis, G. and Pomerantz, D.I. Journal of applied physics, 40(10), pp.3946-3949, 1969.
[2] Dukler, A.E., Hubbard, M.G. Industrial & Eng. Che. Fundamentals, 14(4), 337-347, 1975.
[3] Taitel, Y., & Barnea, D., 1990. Two-phase slug flow. In Advances in heat transfer (Vol. 20, pp. 83-132).
[4] Nicholson, M.K., Aziz, K. and Gregory, G.A. The Canadian J. Che. Eng., 56(6), pp.653-663, 1978.
[5] Fernandes, R., Semiat, R., Dukler, A. AIChE J. 29, 981–989, 1983.
[6] Sylvester, N.D. Trans. ASME 109, 206–213, 1987.
[7] Ishii, M. Multiphase Sc. and technology, 5(1-4), 1990.
[8] Taitel, Y., & Barnea, D. Che. Eng. Sc., 53(11), 2021.
[9] Rosa, E. S., Souza, M. A. Flow Measurement and Instrumentation, 46, 139-154, 2015.
[10] Grigoleto, M.M., Bassani, C.L., Conte, M.G., Cozin, C., Barbuto, F.A., Morales, R.E. Int. J. Heat and Mass Transfer, 165, 120664, 2021.
[11] Van Hout, R., Shemer, L., & Barnea, D. Int. J. Multiphase Flow, 18(6), 831-845, 1992.
[12] Collins, R., de Moraes, F.F., Davidson, J.F., Harrison, D. J. of Fluid Mechanics, 89(3), 1978.
[13] Nogueira, S., Riethmuller, M.L., Campos, J.B.L.M. and Pinto, A.M.F.R., 2006. Che. Eng. Sc., 61(22), pp.7199-7212.
[14] P.A.D. Maldonado, C.C. Rodrigues, E. Mancilla, E.N. dos Santos, M.A.M. Neto, M.J. da Silva, R.E.M. Morales. Exp. Therm. Fluid Sci. 111093, 2023.
[15] Dos Santos, Eduardo N., et al. IEEE Access 7, 5374-5382, 2018.
[16] Barnea, D., Shemer, L. Int. J. of Multiphase Flow, 15(4), 495-504, 1989.